Individual-based quantitative temporal beta-diversity: Novel indices for assessing community compositional shifts accounting for changes in the properties of individuals

Running title: Individual-based quantitative beta-diversity

Ryosuke Nakadai*[1]

ORCID: 0000-0002-9512-8511

[1] Biodiversity Division, National Institute for Environmental Studies, Onogawa 16-2, Tsukuba, Ibaraki, 305-8506, Japan

* Corresponding author: R. Nakadai
E-mail: r.nakadai66@gmai.com, nakadai.ryosuke@nies.go.jp
Biodiversity Division, National Institute for Environmental Studies, Onogawa 16-2, Tsukuba, Ibaraki, 305-8506, Japan

Author contributions

R.N. conceived the study, designed the methods described herein, analysed the empirical data, and wrote the manuscript.

Acknowledgments

Financial support was provided by the Japan Society for the Promotion of Science and a Program of the National Institute for the Environmental Studies, Japan.

Conflicts of interest

The author declares no conflicts of interest.

Data Availability

Data are available from the package rFIA (Stanke et al., 2020) in R, and the code used to calculate the indices introduced in the present study is provided in Supplementary File 1.

Biosketch

Ryosuke Nakadai is a Research Associate at the National Institute for Environmental Studies, Japan, with a broad interest in biodiversity, biological interactions, and ecosystem services across temporal and spatial scales. His work includes analyses of biodiversity patterns and the development of both statistical and molecular tools for a wide range of taxa.

Individual-based quantitative temporal beta-diversity: Novel indices for assessing community compositional shifts explicitly accounting for changes in the properties of individuals

Running title: Individual-based quantitative beta-diversity

Abstract

Aim

Revealing patterns of temporal biodiversity change is an urgent issue in light of the effects of global climate change. In addition, climate change is known to modify not only biodiversity but also individual life-history. Nevertheless, although the connection between individual physiology and large-scale ecological patterns is a major challenge for the mechanistic understanding of macroecology, large gaps exist between individual life-history and biodiversity. In this context, novel methods can be used to evaluate changes in individual properties and their effects on biodiversity.

Innovation

Novel indices that can evaluate compositional shifts across time by explicitly considering the contributions of the life-histories (i.e., growth, mortality, and recruitment) of individuals in a community were successfully developed. By applying subset data of the Forest Inventory and Analysis database for the state of Rhode Island in the USA, changes in the contribution of individual life-histories to biodiversity change were successfully identified.

Main conclusions

The development of the proposed novel indices not only represents methodological progress in community ecology and macroecology but also a conceptual advance, bridging studies of biodiversity and individual life-history and physiology. The individual-based diversity index opens the door to the possibility of individual-based

biodiversity science, which could facilitate understanding the comprehensive effects of climate change across different hierarchies of biological organisation.

Keywords: climate change, compositional shift, life-history, growth, temporal beta diversity

Introduction

Elucidating patterns of biodiversity change over time in light of the effects of global climate change and anthropogenic disturbance has been the focus of much attention (Dornelas et al., 2014; García et al., 2016; Vellend et al., 2013). Classical studies have focused on biodiversity loss (i.e., alpha and gamma diversity), and a lack of knowledge on compositional shifts (i.e., beta diversity) has been highlighted until relatively recently (Dornelas et al., 2014; Magurran et al., 2015, 2019). Within this context, several studies have attempted to quantify compositional shifts in biodiversity, termed temporal beta diversity (Gotelli et al., 2017; Magurran, 2011). Recent studies have developed unique methodologies and concepts for temporal beta diversity based on classical spatial beta diversity research (Gotelli et al., 2021; Legendre, 2019; Shimadzu, et al., 2015; Tatsumi et al., 2021).

Because an individual cannot exist in two places at once, it can persist in the same habitat over time (Magurran et al., 2019). Therefore, individual persistence and turnover are important factors for temporal beta diversity. In fact, some individuals of long-lived species (e.g., trees and vertebrates) persist over the long term, whereas individuals of short-lived species are replaced by conspecifics or individuals of other species (Nakadai, 2020, 2021). In this context, Nakadai (2020) recently proposed the "individual-based beta-diversity" concept to bridge the gap between biodiversity and individual information, and provided novel indices to evaluate individual turnover and compositional shifts based on comparisons between two periods at a given site. Specifically, I developed an individual-based temporal beta-diversity approach for the Bray-Curtis dissimilarity index (i.e., an abundance-based temporal beta-diversity index) (Nakadai, 2020). Subsequently, Nakadai (2020, 2021) added both persistence and turnover of individuals to the compositional shifts in biodiversity across time.

Climate change is known to modify not only biodiversity directly but also the individual life-histories of organisms (Brienen et al., 2020; Searle & Chen, 2018).

Recent studies have shown that climate warming will facilitate faster growth and shorter life spans for individual trees as a physiological process within individuals (Körner, 2017; Munné-Bosch, 2018; Searle & Chen, 2018) and increase the amount of carbon stocks in terrestrial ecosystems (Brienen et al., 2015). As a result, these changes in individual life-history potentially affect the compositional shifts of local communities and, consequently, global biodiversity. Nevertheless, although the connection between individual physiology and large-scale ecological patterns is a major challenge for mechanistic understanding in macroecology (Brown, 1995, 1999; Brown et al. 2004; Hubbell, 2001; e.g., metabolic theory), large gaps still exist between individual life-history and biodiversity. To comprehensively understand the effects of climate change, it is essential to simultaneously capture all the property changes of individuals, individual turnover, and changes in biodiversity.

Despite these needs, the approaches of previous individual-based temporal beta-diversity (Nakadai, 2020, 2021) only take into account the presence or absence of each individual (i.e., qualitative properties such as ‘dead’ or ‘alive’), and the influences of the property changes of each individual (e.g., individual growth) over time on biodiversity have been neglected, which is further influenced by global climate change. Therefore, the purpose of this study was to develop new individual-based temporal beta-diversity indices that can assess compositional shifts across time by explicitly including the property changes of each individual in a community. Hereafter, I call the indices developed in Nakadai (2020) and the novel indices introduced in the present study individual-based “qualitative (QL)” indices and individual-based “quantitative (QT)” indices, respectively. By introducing quantitative individual information (e.g., size and weight), these novel indices can evaluate the contribution of individual growth and the differences between large and small individuals. Thus, after briefly reviewing the history of pairwise beta-diversity indices, I extend individual-based QL temporal beta-diversity indices to QT indices. I then apply these indices to a subset of the Forest

Inventory and Analysis (FIA) database for the state of Rhode Island in the USA (Stanke et al., 2020, Burrill et al., 2021) as a case study to demonstrate their application.

Materials and Methods

Conventional incidence-based and abundance-based indices and recently developed individual-based qualitative (QL) temporal beta-diversity indices

Incidence-based and abundance-based beta-diversity indices have been previously proposed (Baselga, 2013). For example, the widely used Bray-Curtis dissimilarity index (Odum, 1950) is an abundance-based extension of the Sørensen index (Baselga, 2013; Legendre & Legendre, 2012; Sørensen, 1948). Incidence-based methods target the number of species, whereas abundance-based methods mainly target the number of individuals. It should be noted that abundance-based methods sometimes target area, biomass, weight, etc. (e.g., Li et al., 2016). I describe this approach in more detail in the present paper. Conventional beta-diversity indices are based on intersection (A, a) and relative complement (B, b, C, c) components. Hereafter, here I explain only the context of temporal beta diversity. Specifically, the Sørensen dissimilarity index (d_{sor}; Sørensen, 1948) is formulated as follows:

$$d_{sor} = \frac{b+c}{2a+b+c} \qquad \text{equation 1}$$

where a is the number of species common to both temporal units; b is the number of species that occur in the first but not the second unit; and c is the number of species that occur in the second unit but not the first unit. Analogously, the Bray-Curtis dissimilarity index (Odum, 1950) is formulated as follows:

$$d_{BC} = \frac{B+C}{2A+B+C}. \qquad \text{equation 2}$$

As a premise for explanation, assume that there are two sets of community data along the time axis—communities at time *j* and time *k* (abbreviated as T*j* and T*k*: *j* < *k*), respectively. The abundance-based components are as follows.

$$A = \sum_i \min(x_{ij}, x_{ik}) \quad \text{equation 3a}$$

$$B = \sum_i \left[x_{ij} - \min(x_{ij}, x_{ik})\right] \quad \text{equation 3b}$$

$$C = \sum_i \left[x_{ik} - \min(x_{ij}, x_{ik})\right] \quad \text{equation 3c}$$

where x_{ij} is the abundance of species *i* at temporal unit *j*, and x_{ik} is the abundance of species *i* at temporal unit *k*. Therefore, *A* is the number of individuals of each species shared by units *j* and *k*, and *B* and *C* are the numbers of individuals unique to units *j* and *k*, respectively.

Nakadai (2020) introduced the categorisation of the community dynamics component into persistence (*p*), mortality (*m*), and recruitment (*r*) in individual-based temporal beta diversity. *m* refers to individuals occurring at T*j* that die before T*k*, thereby representing the total number of dead individuals during the time between T*j* and T*k*. *r* identifies individuals that were not alive at T*j* (or were not yet in the size class counted) but were subsequently alive and counted at T*k*, thereby representing the total number of recruited individuals between T*j* and T*k*. Component *p* refers to the persistence of individuals from T*j* to T*k*. Note that, unlike previous studies (Nakadai, 2020, 2021: Fig. 1a), I use lower-case letters for the components of individual-based qualitative indices (i.e., *p*, *m*, *r*) to distinguish the components of the individual quantitative indices described later. Thus, the abundances are calculated as follows:

$$p = \sum_o \min(z_{oj}, z_{ok}) \quad \text{equation 4a}$$

$$m = \sum_o \left[z_{oj} - \min(z_{oj}, z_{ok})\right] \quad \text{equation 4b}$$

$$r = \sum_o \left[z_{ok} - \min(z_{oj}, z_{ok})\right], \quad \text{equation 4c}$$

where z_{oj} is individual o at time Tj, and z_{ok} is individual o at time Tk. Both z_{oj} and z_{ok} have values of one or zero (presence and absence, respectively). Therefore, p is the total number of individuals present at both Tj and Tk, and m and r are the numbers of individuals unique to Tj and Tk, respectively (Nakadai, 2020, 2021: Fig. 1a).

This formulation of the individual-based temporal beta-diversity index for the Bray-Curtis (d_{mr}) dissimilarity can be expressed as follows:

$$d_{mr} = \frac{m+r}{2p+m+r} \qquad \text{equation 5}$$

In some cases, there is a turnover of different individuals belonging to the same species, even when the community composition is stable over time. Therefore, the components that change over time (m and r) are reorganised into two further components, namely compositional equilibrium (e) and shift (B and C), respectively (Nakadai, 2020, 2021). Component m can be partitioned into lost individuals that contribute to compositional shifts in a community (B) and lost individuals replaced by conspecifics that contribute to equilibrium in community composition (e_{loss}) (Fig. 1a). Similarly, component r can be partitioned into gained individuals that contribute to compositional shifts in a community (C) and gained individuals that replace conspecifics, thereby contributing to equilibrium in community composition (e_{gain}) (Fig. 1a). By definition, the number of e_{loss} and e_{gain} individuals is identical; thus, I replaced both e_{loss} and e_{gain} with the coefficient e (Nakadai, 2020, 2021). Furthermore, components m and r can be analysed in the same manner as the community data (Nakadai, 2020). Therefore, the Bray-Curtis dissimilarity between communities can be calculated based on m and r as follows:

$$v_{s.QL} = \frac{B+C}{2e+B+C} = \frac{B+C}{m+r} \qquad \text{equation 6}$$

where $v_{s.QL}$ indicates the speed of compositional shifts in a community relative to the total speed of individual turnover associated with *m* and *r*. It is also possible to calculate $v_{s.QL}$ as d_{BC} divided by d_{mr}, as follows:

$$d_{BC} \div d_{mr} = \frac{B+C}{2A+B+C} \div \frac{m+r}{2p+m+r} = \frac{B+C}{2(p+e)+B+C} \div \frac{m+r}{2p+m+r} = \frac{B+C}{2o+m+r} \div \frac{m+r}{2p+m+r} = \frac{B+C}{2e+B+C} = v_{s.QL}. \quad \text{equation 7}$$

Novel individual-based "qualitative (QT)" beta-diversity indices

I developed individual-based QT components and novel indices for community datasets over time using individual property information (e.g., size and weight). The relationship between the QL and QT indices is similar to that between the incident-based and abundance-based indices. In other words, individual-based QT components were calculated as individual-based QL weighted by individual properties. As previously noted, the abundance targeted by abundance-based indicators is not necessarily the number of individuals but can also include area, volume, etc. Abundance except for the number of individuals for community datasets has been used in cases of large size variation among individuals within a community or where it is difficult to recognise proper individuals (Li et al., 2016). Hereafter, the Bray-Curtis indices targeting measures except the number of individuals (e.g., sizes and weights) are described as $d_{BC'}$ and their components are described with apostrophes (*A'*, *B'*, and *C'*) to distinguish the unweighted Bray-Curtis index as follows:

$$d_{BC'} = \frac{B'+C'}{2A'+B'+C'}. \quad \text{equation 8}$$

This weighting indicates that abundance-based (number of individual-based) diversity indices were weighted by total measures of individuals for each species,

thus calculating diversity indices by considering the variation of measures of each individual implicitly. Because individuality is rarely clearly identifiable in weighted indices, this relationship is not well recognised.

In addition to individual-based QL indices, individual-based QT indices comprise components of mortality and recruitment (*M* and *R*, respectively). In the QT indices, *M* refers to the total number of measures of individuals occurring at T*j* that die before T*k*, thereby representing the total number of measures of the mortal individuals between T*j* and T*k* (Fig. 1b). *R* identifies the total number of measures of individuals that were not alive at T*j* (or were not yet in the size class counted) but were subsequently alive and counted at T*k*, thereby representing the total number of measures of the recruited individuals between T*j* and T*k* (Fig. 1b).

From this point on, the major differences between the QL and QT indices are as follows. The persistent individuals are qualitatively identical, thus keeping their alive (or present) status between T*j* and T*k*, but rarely maintain the same status in terms of size and weight; thus, there is a change in individual properties between T*j* and T*k*. For example, in tree communities, one newly recruited small tree can be a large tree after the persistence of half a century. In the *p* component of QL indices, this means that an individual is persistent, while it is impossible to evaluate changes in the features (i.e., basal area, biomass, and/or weight, etc.) of the individual. The indices introduced here overcome this problem by considering the contribution of changes in individual properties, mainly targeting individual growth. Specifically, in the case of persistent individuals, the original and altered total number of measures are partitioned into persistent (*P*) and growth (*G*) components, respectively. Thus, the respective total number of measures of the components were calculated as follows:

$$M = \sum_o \left[w_{oj} - \min\left(w_{oj}, w_{ok}\right) \times \left[z_{oj} - \min\left(z_{oj}, z_{ok}\right)\right]\right] \qquad \text{equation 9a}$$

$$R = \sum_o \left[\left[w_{ok} - \min\left(w_{oj}, w_{ok}\right)\right] \times \left[z_{ok} - \min\left(z_{oj}, z_{ok}\right)\right]\right] \qquad \text{equation 9b}$$

$$P = \sum_o \min\left(w_{oj}, w_{ok}\right) \qquad \text{equation 9c}$$

$$G = \sum_o \left[\left[\max(w_{oj}, w_{ok}) - \min(w_{oj}, w_{ok})\right] \times \min(z_{oj}, z_{ok})\right]$$ equation 9d,

where w_{oj} is the measure of individual o at time Tj, and w_{o2} is the measure of individual o at time Tk. M and R are the total number of measures of mortal and recruited individuals, respectively. The persistent and growth parts represent the unchanged and changed parts of measures within an individual between Tj and Tk, respectively. Thus, P and G represent the total amount of these components within a community. Equation 9d also considers decreasing changes in the measures of each individual. Therefore, the calculation of the G component can be partitioned into increasing and decreasing parts, as follows:

$$G = \sum_o \left[\left[\max(w_{oj}, w_{ok}) - \min(w_{oj}, w_{ok})\right] \times \min(z_{oj}, z_{ok})\right] = G_{in} + G_{de}$$ equation 10,

where G_{in} and G_{de} are the total increased and decreased parts of the targeted measures, respectively. Specifically, the formulas for G_{in} and G_{de} are as follows:

$$G_{in} = \sum_o \left[\left[w_{ok} - \min(w_{oj}, w_{ok})\right] \times \min(z_{oj}, z_{ok}) \times \frac{1}{2}\left[1 + \mathrm{sign}(w_{ok} - w_{oj})\right]\right]$$ equation 11a

$$G_{de} = \sum_o \left[\left[w_{oj} - \min(w_{oj}, w_{ok})\right] \times \min(z_{oj}, z_{ok}) \times \frac{1}{2}\left[1 - \mathrm{sign}(w_{ok} - w_{oj})\right]\right]$$ equation 11b,

where $\frac{1}{2}\left[1 + \mathrm{sign}(w_{ok} - w_{oj})\right]$ and $\frac{1}{2}\left[1 - \mathrm{sign}(w_{ok} - w_{oj})\right]$ distinguish the large and small relationships between w_{ok} and w_{oj} by returning 1 or 0.

This formulation of the individual-based QT temporal beta-diversity index for Bray-Curtis dissimilarity (d_{MRG}) can be expressed as follows:

$$d_{MRG} = \frac{M+R+G}{2P+M+R+G}. \qquad \text{equation 12}$$

Furthermore, this individual-based QT temporal beta diversity can be partitioned into the relative contributions of mortality (d_M), recruitment (d_R), and growth (d_G) to the target weights or measurements, as follows:

$$d_{MRG} = \frac{M+R+G}{2P+M+R+G}$$
$$= \frac{M}{2P+M+R+G} + \frac{R}{2P+M+R+G} + \frac{G}{2P+M+R+G} = d_M + d_R + d_G. \qquad \text{equation 13}$$

In addition, as shown in equations 11a and b, the G component can be partitioned into G_{de} and G_{in}, which are the total decrease and increase, respectively, in the targeted measures. Equation 13 can then be partitioned into two components, as follows:

$$d_{MRG} = \frac{M+R+G}{2P+M+R+G}$$
$$= \frac{M+G_{de}}{2P+M+R+G} + \frac{R+G_{in}}{2P+M+R+G} = d_{de} + d_{in}. \qquad \text{equation 14}$$

where d_{de} and d_{in} indicate the contributions of the decrease and increase, respectively, to the total changes in the targeted measures in T*j* and T*k*. In addition to the QL indices (Nakadai, 2020, 2021), the components that change over time (*M*, *R*, and *G*) can be reorganised into two components—compositional equilibrium (*E*) and shift (*B'* and *C'*), respectively. Components $M + G_{de}$ can be reorganised as the total number of lost measures that contribute to compositional shifts in a community (*B'*) and the total number of lost measures replaced by conspecifics, contributing to the equilibrium in community composition (E_{loss}) (Fig. 1b). Similarly, component $R + G_{in}$ can be reorganised as the total number of measures that contribute to compositional shifts in a community (*C'*) and the total number of gained measures replacing conspecifics,

contributing to equilibrium in community composition (E_{gain}) (Fig. 1b). By definition, the total amount of E_{loss} and E_{gain} are identical; hence, I replaced both E_{loss} and E_{gain} with coefficient E.

$$d_{MRG} = \frac{M+R+G}{2P+M+R+G} = \frac{M+G_{de}}{2P+M+R+G} + \frac{R+G_{in}}{2P+M+R+G}$$
$$= \frac{E+B}{2P+M+R+G} + \frac{E+C}{2P+M+R+G} = \frac{2E}{2P+M+R+G} + \frac{B+C}{2P+M+R+G} = d_S + d_E.$$

equation 15

Furthermore, components M, R, and G (i.e., $M + G_{de}$ and $R + G_{in}$) can be analysed in the same manner as the community data. Therefore, the Bray-Curtis dissimilarity between communities (i.e., the total amount of lost and gained measures) can be calculated based on M, R, and G, as follows:

$$v_{s.QT} = \frac{B'+C'}{2E+B'+C'} = \frac{B'+C'}{M+R+G}$$ equation 16

where $v_{s.QT}$ indicates the relative speed of compositional shifts in a community against the total turnover of targeted measures associated with M, R, and G. If $v_{s.QT}$ is 0, then the turnover of the targeted measures would not contribute to compositional shifts in a community. If $v_{s.QT}$ is 1, all turnover of the targeted measures contributes to the compositional shifts. It is also possible to calculate $v_{s.QT}$ as $d_{BC'}$ divided by d_{MRG}, as follows:

$$d_{BC'} \div d_{MRG} = \frac{B'+C'}{2A'+B'+C'} \div \frac{M+R+G}{2P+M+R+G} = \frac{B'+C'}{2(P+E)+B'+C'} \div \frac{M+R+G}{2P+M+R+G} = \frac{B'+C'}{2P+M+R+G} \div \frac{M+R+G}{2P+M+R+G} = \frac{B'+C'}{M+R+G} = v_{s.QT}.$$ equation 17

Here, I have only focused on an extension of Bray-Curtis dissimilarity. In Supplementary Text 1, I also summarise individual-based beta diversity using the

Ružička dissimilarity index (Ružička, 1958), which was identified by Podani et al. (2013) and Legendre (2014) as an appropriate index for beta diversity studies. The Ružička dissimilarity index is an abundance-based extension of the Jaccard dissimilarity index (Jaccard, 1901). Nevertheless, I recommend using the Bray-Curtis family of indices in individual-based temporal beta diversity because the formulations based on these indices are simpler than the Ružička indices, especially with respect to the derivation $v_{s.QL}$ and $v_{s.QT}$.

Case study: Subset of the Forest Inventory and Analysis (FIA) database for the state of Rhode Island in the USA

As a case study application of the new individual-based QT indices based on publicly available data, here I focus on a subset of data from the United States Department of Agriculture Forest Service's FIA Program for the state of Rhode Island using the R package rFIA (Stanke et al., 2020). The FIA database is a well-known dataset that includes individual tree tracking and size information (i.e., basal area and bole biomass). A comprehensive summary of the associated data and sampling methodology is provided by Burrill et al. (2021). Briefly, each FIA plot comprises four 0.017-ha circular subplots, each located within a circular 0.10 ha macroplot. All free-standing woody stems (alive and dead) with a diameter of ≥ 12.7 cm were sampled within each subplot (Burrill et al., 2021).

The original dataset included 10,093 individual-time records for 58 species, including multiple species (spp.) in 140 plots from 2004 to 2018. Some plots included more than two surveys, for which it was possible to calculate more than one value of temporal beta diversity. I conducted plot-level filtering of the dataset using the following criteria: (1) those with unidentified individuals at the species level were excluded; (2) those with ten individuals or more were included; and (3) a survey interval between two surveys of 5 ± 1 years was targeted. In addition, individual trees

with a 12.7-cm diameter at breast height (DBH) and above were targeted because the bole biomass was also estimated. The final dataset included 5,705 individual-time records comprising 2,541 individual trees of 32 species across 126 survey intervals (86 unique plots). The latitudinal and longitudinal ranges in the dataset are N 41.39446°–42.00797° and 71.79635°–71.12814°W, respectively. The elevation range was 10–680 m. The geographical location of each plot is shown in Fig. S1.

I focused on the basal area and bole biomass of each tree as changes in individual properties that can be considered in the novel indices developed in the previous sections. The basal areas of live trees were calculated as $\frac{DIA}{2} \times \frac{DIA}{2} \times \pi$. The gross cubic-foot volume of the live trees was estimated at ≥ 12.7 cm DBH, which defined the total volume of wood in the central stem of the inventoried trees (bole biomass) assuming a 30.48-cm mean stump height and a minimum 10.16 cm top diameter (for detailed estimation method see Domke et al., 2013).

To demonstrate the application of the novel indices, I focused mainly on the following 11 indices: d_{BC}, d_{mr}, d_m, d_r, $v_{s.QL}$, $d_{BC'}$, d_{MRG}, d_M, d_R, d_G, and $v_{s.QT}$. Formulas of the base indices (i.e., d_{BC}, d_{mr}, $v_{s.QL}$, $d_{BC'}$, d_{MRG}, and $v_{s.QT}$) are summarised in Table 1. All 11 indices were calculated for each survey interval for each plot. For the latter six indices (i.e., $d_{BC'}$, d_{MRG}, d_M, d_R, d_G, and $v_{s.QT}$) were calculated for both basal area and bole biomass, and I added "_area" or "_biomass" to distinguish them, respectively. First, I tested the relationships among d_{BC}, d_{mr}, $v_{s.QL}$, $d_{BC'}$, d_{MRG}, and $v_{s.QT}$ using simple linear regression. Second, to reveal the geographical and temporal components of the indices, I constructed models using linear mixed models and linear models for each index. As explanatory variables, geographic factors (latitude and elevation), a temporal factor (mean calendar year between the first and second surveys), and a sampling-design-related factor (length of survey interval) were used. Plot identity was considered a random effect in the model comparisons because 40 plots included two survey intervals. However, the model comparisons showed that the linear mixed models

always had higher Akaike information criterion (AIC; Akaike, 1998) values than the linear model (Table S1). Thus, all of the results shown in the following discussion are based on linear models.

All analyses were conducted using R software (ver. 4.1.0; R Development Core Team, 2021). The R packages *vegan* (Oksanen et al., 2020), *nlme* (Pinheiro et al., 2022), and *MuMIn* (Barton, 2022) were used to convert the abundance data to presence-absence data, construct a linear mixed model, and model comparisons based on AIC. The R scripts used to calculate the new indices are provided in Supplementary File 1.

Results

Among 126 survey intervals, the individual turnover of 10 survey intervals was zero, which were subsequently excluded from the targets when calculating the $v_{s.QL}$ indices. The distribution of the novel indices, except $v_{s.QT}$, is shown in Fig. 2. The d_{MRG} indices based on both basal area and bole biomass were strongly and positively correlated with d_{BC}, d_{mr}, area-based $d_{BC'}$, and biomass-based $d_{BC'}$ (≥ 0.87; Fig. S3). On the other hand, the $v_{s.QT}$ indices based on both basal area and bole biomass were only weakly correlated with the $d_{BC'}$ indices based on both basal area and bole biomass (r = 0.23–0.28, Fig. S3) and showed no correlation with $v_{s.QL}$ (r = 0.16 and 0.08, Fig. S3). For both d_{MRG} and $v_{s.QT}$, strong correlations existed between the indices based on basal area and bole biomass (r = 0.99 and 0.91, Fig. S3). All the Pearson correlation coefficients are summarised in Fig. S3.

As a result of AIC comparison, null models were chosen for the three indices, i.e., the indices for compositional shift based on number of individuals and basal area (d_{BC}, $d_{BC'_area}$) and the relative speed of compositional shift against total changes in basal area ($v_{s.QT_area}$) (Table 2). The index of compositional shift based on bole biomass ($d_{BC'_biomass}$) tended to increase with longer survey intervals as a result of model comparison (Table 2). In the index for the relative speed of compositional shift against

total individual turnover ($v_{s.QL}$), only elevation was chosen as an explanatory variable based on the AIC comparison; thus, the index increased toward higher elevations (Table 2). For the relative speed of compositional shift against total changes in basal area ($v_{s.QT_biomass}$), a model including calendar year and survey interval was chosen by the AIC comparison (Table 2); specifically, the index increased toward older calendar years and longer survey intervals. In both indices of the total amount of change in basal area and bole biomass (d_{MRG_area}, $d_{MRG_biomass}$), models with latitude and survey interval were chosen as the best models in the AIC comparisons (Table 2); specifically, the indices tended to be higher toward lower latitudes and with longer survey intervals. On the other hand, in the index of total individual turnover (d_{mr}), the model with only the survey interval was chosen as the best model (Table 1), increasing toward longer survey intervals. In the three indices related to the contribution of mortality to the total amount of change (d_m, d_{M_area}, $d_{M_biomass}$), models with latitude and calendar year were chosen as the best models (Table 2), tending to be higher toward lower latitudes and more recent years. In the indices related to the contribution of recruitment to the total amount of change (d_{R_area}, $d_{R_biomass}$), models with calendar year were selected as the best models (Table 2), tending to be higher toward less recent years. In addition, in the index related to the contribution of recruitment to the total individual turnover (d_r), the model with calendar year and survey interval was chosen as the best model (Table 2), with the index tending to be higher toward less recent years and at longer survey intervals. For both indices related to the contribution of growth to the total amount of change (d_{G_area}, $d_{G_biomass}$), models were chosen that included the survey interval and, in the case of basal area, calendar year.

Discussion

The potential for evaluating the contributions of individuals' persistence to compositional shifts in a community was first proposed by Nakadai (2020). Here, I

extended the previously established individual-based beta-diversity approaches (Nakadai, 2020, 2021) to take account of individual property changes—even for persistent individuals—that are not currently considered in qualitative indices. Specifically, in addition to the components of mortality and recruitment as considered in Nakadai (2020), I introduced a growth component to account for the property changes individuals in the context of compositional shifts for the first time. Thus, the novel indices proposed here not only represent methodological progress in community ecology and macroecology but also provide a conceptual advance bridging biodiversity and individual life-history and physiology studies.

To illustrate the application of the novel indices, I applied these to a subset of the FIA database for the state of Rhode Island in the USA. This analysis demonstrated that the contribution of tree growth to the total turnover of both basal area and bole biomass was generally larger than that of mortality and recruitment (Fig. 2a, b: Fig. S2). This suggests the importance of previously overlooked growth factors in forest turnover and dynamics as well as subsequent compositional shifts. In the case study dataset, the calculated abundance-based and individual-based indices (i.e., d_{BC}, d_{mr}, $d_{BC'}$, and d_{MRG}) were strongly correlated. Thus, iff the contribution of individual tree growth is high, the strength of the correlation between d_{mr} and d_{MRG} should decrease, yet this was not the case. On the other hand, I found no clear relationships between the $v_{s.QL}$ index and $v_{s.QT}$ indices based on both basal area and bole biomass and the relative speed of compositional shift. Generally, the values of $v_{s.QL}$ for the FIA dataset are high; thus, individual turnover generally contributed to compositional shift, although both $v_{s.QT_area}$ and $v_{s.QT_biomass}$ were lower and more variable than $v_{s.QL}$. These results reflect the differences in the characteristics of the novel quantitative indices developed here and the conventional qualitative index. Indeed, $v_{s.QL}$ could not be applied to 10 plots that had no individual turnover, whereas, in such cases, the $v_{s.QT}$ index is more sensitive than the $v_{s.QL}$ index to temporal changes in the community.

In the driver analysis of the calculated indices, I found that various explanatory variables affected the results. First, focusing on the growth component specific to the new quantitative index, both area- and biomass-based d_G indices, which indicate the contribution of growth, were responsive to the survey interval. This strongly suggests an accurate evaluation of the contribution of growth was achieved. In addition, the area-based d_G index tended to decrease toward a larger (i.e., more recent) calendar year. In addition, overall, the contributions related to recruitment decreased, and those related to mortality increased (Table 2), which may be indicative of succession (i.e., aging forests) and/or climate change.

The $v_{s.QT_area}$ index showed no clear pattern due to the null model selected, whereas the $v_{s.QL}$ and $v_{s.QT_biomass}$ indices varied with elevation and calendar year, respectively. The v_s family of indices is designed to capture changes that take account of stochastic changes, such as individual, basal area, or bole volume turnover. This suggests that along with the explanatory variables, niche processes drive compositional shifts, which cannot be explained by stochastic processes alone. For example, Nakadai (2020) showed that $v_{s.QL}$ values vary along climate gradients (i.e., the change ratio of annual mean temperature) for both deciduous and evergreen broadleaf forests.

Although the indices I have introduced here are mainly applicable to datasets containing both individual identity and property information, a method that accommodates various types of quantitative individual information may become available through future technological developments. Generally, information for individuals remains limited in community ecology and macroecology, yet in the era of big data, this is likely to be addressed in the near future. In addition, if the contributions of demographic factors (i.e., growth, mortality, and recruitment) can be estimated using hierarchical modelling approaches (e.g., Hill et al., 2004, Kanamori et al., 2017), these indices could be calculated even in the absence of detailed individual-tracking information.

Notably, climate change affects various ecological hierarchies, from global biodiversity to individuals and even intra-individual phenomena (Arneth et al., 2020; Körner, 2017). Applying the individual-based beta-diversity indices to global datasets, especially forest inventory data (e.g., ForestGEO; https://forestgeo.si.edu/), is, therefore, highly promising for assessing the impacts of global climate change. Indeed, individual-based diversity indices able to account for previously overlooked elements of biodiversity, such as individual persistence and growth, open the door to innovative individual-based biodiversity science. This should facilitate a greater understanding of the effects of climate change across multiple hierarchies of biological organisation.

Data Availability Statement

Data are available from the package rFIA (Stanke et al., 2020) in R, and the code used to calculate the indices introduced in the present study is provided in Supplementary File 1.

References

Akaike, H. (1998). Information theory and an extension of the maximum likelihood principle. In E. Parzen, K. Tanabe, and G. Kitagawa (Eds.), *Selected Papers of Hirotugu Akaike* (pp. 199–213). New York, NY. doi:10.1007/978-1-4612-1694-0_15

Arneth, A., Shin, Y. J., Leadley, P., Rondinini, C., Bukvareva, E., Kolb, M., . . . Saito, O. (2020). Post-2020 biodiversity targets need to embrace climate change. *Proceedings of the National Academy of Sciences*, *117*(49), 30882–30891. doi:10.1073/pnas.2009584117

Bartoń, K. (2020). MuMIn: Multi-model inference. R package version 1.43.17. Retrieved from https://CRAN.R-project.org/package=MuMIn

Baselga, A. (2013). Separating the two components of abundance-based dissimilarity: balanced changes in abundance vs. abundance gradients. *Methods in Ecology and Evolution*, *4*, 552–557. doi:10.1111/2041-210X.12029

Brienen, R. J. W., Caldwell, L., Duchesne, L., Voelker, S., Barichivich, J., Baliva, M., . . . Gloor, E. (2020). Forest carbon sink neutralized by pervasive growth-lifespan trade-offs. *Nature Communications, 11*, 4241. https://doi.org/10.1038/s41467-020-17966-z

Brienen, R., Phillips, O., Feldpausch, T. Gloor, E., Baker, T., Lloyd, J., . . . Zagt, R. J. (2015). Long-term decline of the Amazon carbon sink. *Nature*, *519*, 344–348. https://doi.org/10.1038/nature14283

Brown, J. H., Gillooly, J. F., Allen, A. P., Savage, V. M., & West, G. B. (2004). Toward a metabolic theory of ecology. *Ecology, 85*(7), 1771–1789. doi:10.1890/03-9000

Brown, J. H. (1995). *Macroecology*. University of Chicago Press.

Brown, J. H. (1999). Macroecology: Progress and prospect. *Oikos*, 87, 3–14. doi:10.2307/3546991

Burrill, E. A., DiTommaso A. M., Turner, J. A., Pugh, S. A., Menlove, J., Christiansen, G., Perry, C. J., & Conkling, B. L. (2021). *The forest inventory and analysis database: Database description and user guide version 9.0.1 for Phase 2*. U.S. Department of Agriculture, Forest Service (p. 1026). Retrieved from http://www.fia.fs.fed.us/library/database-documentation/

Domke, G. M., Oswalt, C. M., Woodall, C. W., & Turner, J. A. (2013). Estimation of merchantable bole volume and biomass above sawlog top in the National Forest Inventory of the United States. *Journal of Forestry*, *111*(6), 383–387. doi:10.5849/jof.13-042

Dornelas, M., Gotelli, N. J., Mcgill, B., Shimadzu, H., Moyes, F., Sievers, C., & Magurran, A. E. (2014). Assemblage time series reveal biodiversity change but

not systematic loss. *Science*, *344*, 296–299. doi:10.1126/science.1248484

García Molinos, J., Halpern, B. S., Schoeman, D. S., Brown, C. J., Kiessling, W., Moore, P. J., . . . Burrows, M. T. (2016). Climate velocity and the future global redistribution of marine biodiversity. *Nature Climate Change, 6*, 83–88. doi:10.1038/nclimate2769

Gotelli, N. J., Shimadzu, H., Dornelas, M., McGill. B., Moyes. F., & Magurran, A. E. (2017). Community-level regulation of temporal trends in biodiversity. *Science Advances, 3,* e1700315. doi:10.1126/sciadv.1700315

Hill, M. F., Witman, J. D., Caswell, H. (2004). Markov chain analysis of succession in a rocky subtidal community. *The American Naturalist, 164*, 46–61. doi:10.1086/422340

Hubbell, S. P. (2001). *The unified neutral theory of biodiversity and biogeography*. Princeton University Press.

Kanamori Y., Fukaya, K., & Noda, T. (2017). Seasonal changes in community structure along a vertical gradient: Patterns and processes in rocky intertidal sessile assemblages. *Population Ecology, 59*, 301–313. doi:10.1007/s10144-017-0596-z

Körner, C. (2017). A matter of tree longevity. *Science, 355*, 130–131. doi:10.1126/science.aal2449

Legendre, P., & Legendre, L. (2012). Numerical ecology (3rd ed.). Amsterdam: Elsevier.

Legendre, P. (2019). A temporal beta-diversity index to identify sites that have changed in exceptional ways in space–time surveys. *Ecology and Evolution, 9*, 3500–3514. doi:10.1002/ece3.4984

Li, S. P., Cadotte, M. W., Meiners, S. J., Pu, Z., Fukami, T., & Jiang, L. (2016). Convergence and divergence in a long-term old-field succession: The importance of spatial scale and species abundance. *Ecology Letters, 19*(9),

1101–1109. doi:10.1111/ele.12647

Magurran, A. E. (2011). Measuring biological diversity in time (and space). In A. Magurran & B. J. McGill (Eds.), *Biological diversity: Frontiers in measurement and assessment* (pp. 85–104). Oxford: Oxford University Press.

Magurran, A. E., Dornelas, M., Moyes, F., & Henderson, P. A. (2019). Temporal β diversity: A macroecological perspective. *Global Ecology and Biogeography, 28*, 1949–1960. doi:10.1111/geb.13026

Magurran, A. E., Dornelas, M., Moyes, F., Gotelli, N. J., & McGill, B. (2015). Rapid biotic homogenization of marine fish assemblages. *Nature Communication, 6*, 8405. doi:10.1038/ncomms9405

Munné-Bosch, S. (2018). Limits to tree growth and longevity. *Trends in Plant Science, 23*, 985–993. doi:10.1016/j.tplants.2018.08.001

Nakadai, R. (2020). Degrees of compositional shift in tree communities vary along a gradient of temperature change rates over one decade: Application of an individual-based temporal beta-diversity concept. *Ecology and Evolution, 10*(24), 13613–13623. doi:10.1002/ece3.6579

Nakadai, R. (2021). Individual-based multiple-unit dissimilarity: novel indices and null model for assessing temporal variability in community composition. *Oecologia, 197*(2), 353–364. doi:10.1007/s00442-021-05025-3

Odum, E. P. (1950). Bird populations of the Highlands (North Carolina) Plateau in relation to plant succession and avian invasion. *Ecology, 31*, 587–605. doi:10.2307/1931577

Oksanen, J., Guillaume, B. F., Michael, F., Roeland, K., Pierre, L., Dan, M., . . . Helene, W. (2020). Vegan: Community ecology package. R package version 2.5-7. Retrieved from https://CRAN.R-project.org/package=vegan

Pinheiro, J., Bates, D., DebRoy, S., Sarkar, D., & R Core Team. (2022). Nlme: Linear and nonlinear mixed effects models. R package version 3.1-155. Retrieved from

https://CRAN.R-project.org/package=nlme

R Development Core Team. (2021). R: A language and environment for statistical computing. R Foundation for Statistical Computing, Vienna, Austria. (ver. 4.1.0). Retrieved from http://www.R-project.org/

Searle, E. B., & Chen, H. Y. (2018). Temporal declines in tree longevity associated with faster lifetime growth rates in boreal forests. *Environmental Research Letters, 13*(12), 125003. doi:10.1088/1748-9326/aaea9e

Shimadzu, H. et al. (2015). Measuring temporal turnover in ecological communities. *Methods in Ecology and Evolution, 6*, 1384–1394. doi:10.1111/2041-210X.12438

Sørensen, T. A. (1948). A method of establishing groups of equal amplitude in plant sociology based on similarity of species content and its application to analyses of the vegetation on Danish commons. *Biologiske Skrifter, 5(4)*, 1–34.

Stanke, H., Finley, A. O., Weed, A. S., Walters, B. F., & Domke, G. M. (2020). rFIA: An R package for estimation of forest attributes with the US Forest Inventory and Analysis database. *Environmental Modelling & Software, 127*, 104664. doi:10.1016/j.envsoft.2020.104664

Tatsumi, S., Iritani, R., & Cadotte, M. W. (2021). Temporal changes in spatial variation: Partitioning the extinction and colonisation components of beta diversity. *Ecology Letters, 24*(5), 1063–1072. doi:10.1111/ele.13720

Vellend, M., Baeten, L., Myers-Smith I. H., Elmendorf, S. C., Beauséjour, R., Brown C. D., . . . Wipf, S. (2013). Global meta-analysis reveals no net change in local-scale plant biodiversity over time. *PNAS, 110*, 19456–19459. doi:10.1073/pnas.1312779110

Legends

Figure 1 Schematic representation of individual-based temporal beta-diversity for both qualitative (a) and quantitative (b) components. T1 and T2 refer to the communities at times 1 and 2, respectively. Both communities T1 and T2 comprise four species (sp. 1, 2, 3, and 4) and all individuals are identified separately (Z_o) in both cases. The arrows indicate the temporal trajectory for each individual. In the qualitative component (a), *m* refers to individuals in existence at T1 but dead before T2, thereby separately identifying the deaths of individuals during the period between T1 and T2; *r* identifies individuals that were not alive at T1 but found at T2, thereby identifying the recruitment of individuals during the period between T1 and T2; *p* refers to individuals that persisted from T1 to T2, thus both T1 and T2 = 1. In the qualitative component (b), *M* refers to the total amount of measures of individual occurring at T1 that die before T2, thereby representing the total measures of the mortal individuals during the time between T1 and T2; *R* identifies the total measures of individuals that were not alive at T1 but were subsequently alive and counted at T2, thereby representing the recruit individuals between T1 and T2. Persistent individuals are qualitatively identical, having alive (or present) status between T1 and T2, but rarely keep the same status with respect to size and weight. Therefore, change in individual properties occurs between T1 and T2. The quantitative indices consider the contribution of changes of individuals' properties, mainly targeting individual growth. Specifically, for persistent individuals, the original and altered total measures are partitioned into persistent (*P*) and growth (*G*) components, respectively.

Figure 2

Density plots representing the distribution of individual-based quantitative beta-diversity indices across 126 survey intervals for 86 plots (data from Stanke et al. 2020). In all four plots, the values of the indices are limited to the range 0–0.15 to

enable comparison (see Fig. S2 for a plot of the entire range). The plots (a) and (c) are based on basal area, and plots (b) and (d) are based on bole biomass.

Figure 1

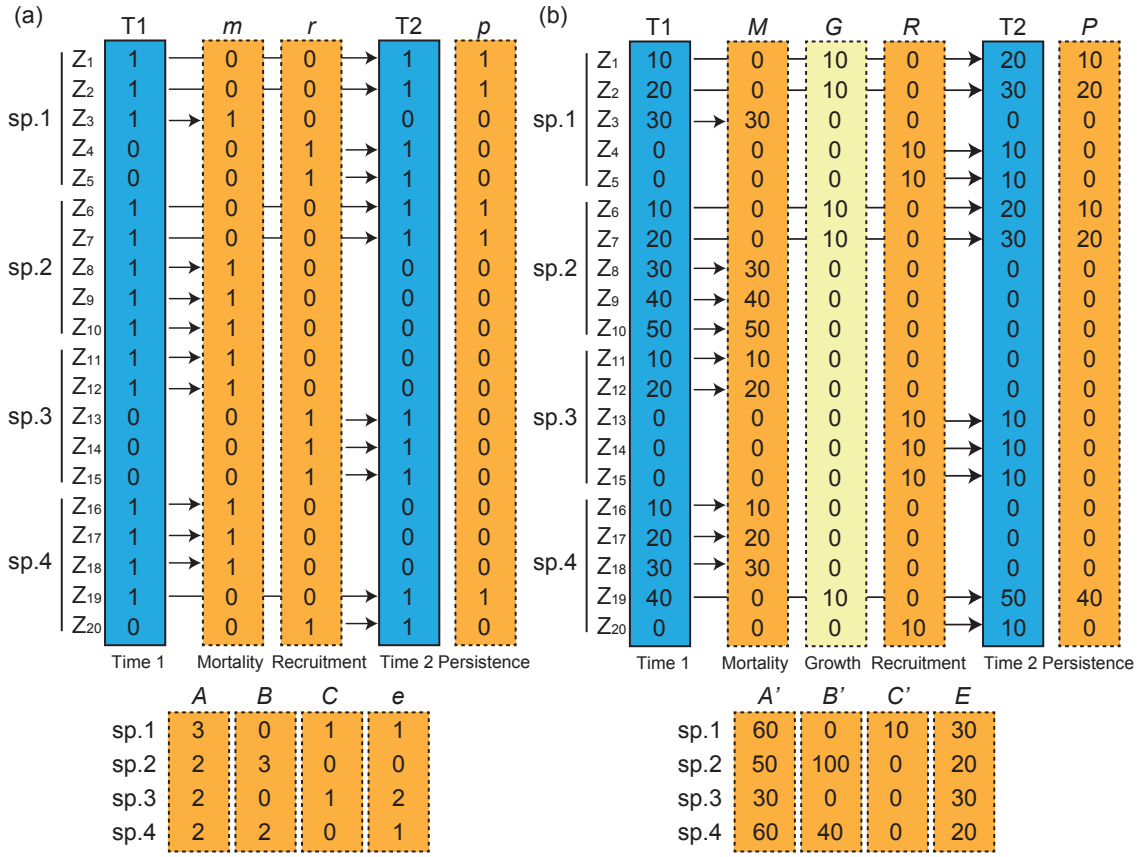
(a)
T1
m
r
T2
p
sp.1
sp.2
sp.3
sp.4
Z1 1 0 0 1 1
Z2 1 0 0 1 1
Z3 1 1 0 0 0
Z4 0 0 1 1 0
Z5 0 0 1 1 0
Z6 1 0 0 1 1
Z7 1 0 0 1 1
Z8 1 1 0 0 0
Z9 1 1 0 0 0
Z10 1 1 0 0 0
Z11 1 1 0 0 0
Z12 1 1 0 0 0
Z13 0 0 1 1 0
Z14 0 0 1 1 0
Z15 0 0 1 1 0
Z16 1 1 0 0 0
Z17 1 1 0 0 0
Z18 1 1 0 0 0
Z19 1 0 0 1 1
Z20 0 0 1 1 0
Time 1
Mortality
Recruitment
Time 2
Persistence
A B C e
sp.1 3 0 1 1
sp.2 2 3 0 0
sp.3 2 0 1 2
sp.4 2 2 0 1
(b)
T1
M
G
R
T2
P
sp.1
sp.2
sp.3
sp.4
Z1 10 0 10 0 20 10
Z2 20 0 10 0 30 20
Z3 30 30 0 0 0 0
Z4 0 0 0 10 10 0
Z5 0 0 0 10 10 0
Z6 10 0 10 0 20 10
Z7 20 0 10 0 30 20
Z8 30 30 0 0 0 0
Z9 40 40 0 0 0 0
Z10 50 50 0 0 0 0
Z11 10 10 0 0 0 0
Z12 20 20 0 0 0 0
Z13 0 0 0 10 10 0
Z14 0 0 0 10 10 0
Z15 0 0 0 10 10 0
Z16 10 10 0 0 0 0
Z17 20 20 0 0 0 0
Z18 30 30 0 0 0 0
Z19 40 0 10 0 50 40
Z20 0 0 0 10 10 0
Time 1
Mortality
Growth
Recruitment
Time 2
Persistence
A' B' C' E
sp.1 60 0 10 30
sp.2 50 100 0 20
sp.3 30 0 0 30
sp.4 60 40 0 20

Figure 2

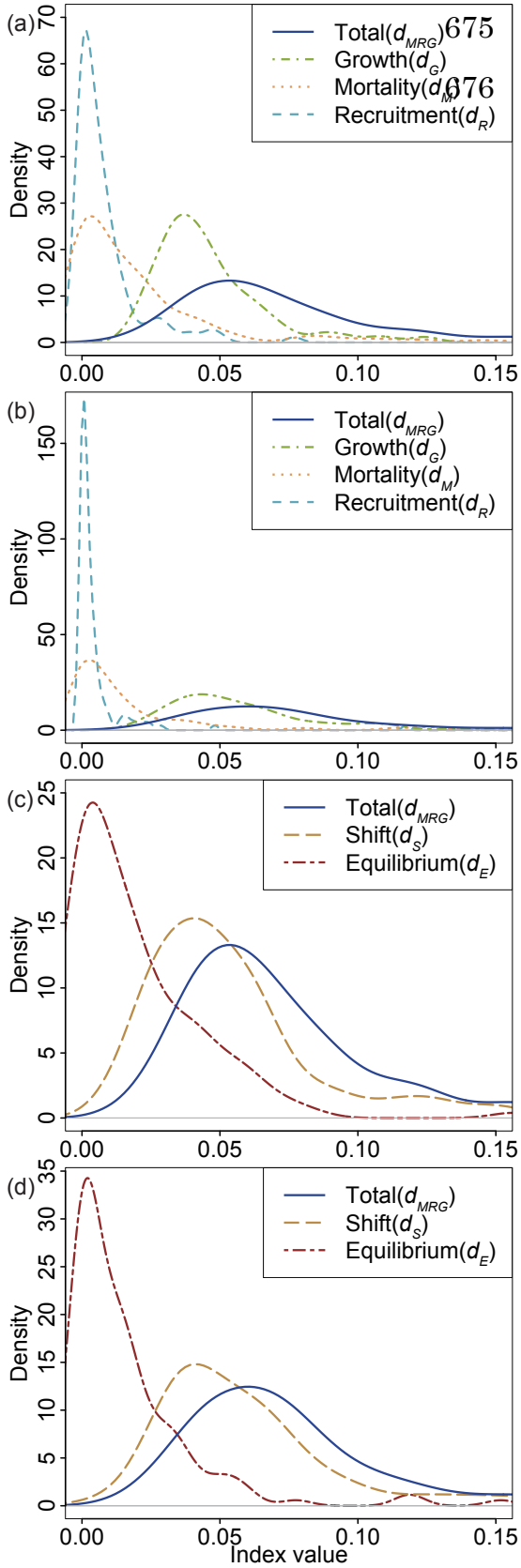
(a)
Total(d_{MRG})
Growth(d_G)
Mortality(d_M)
Recruitment(d_R)
Density
0
10
20
30
40
50
60
70
0.00
0.05
0.10
0.15
(b)
Total(d_{MRG})
Growth(d_G)
Mortality(d_M)
Recruitment(d_R)
Density
0
50
100
150
0.00
0.05
0.10
0.15
(c)
Total(d_{MRG})
Shift(d_S)
Equilibrium(d_E)
Density
0
5
10
15
20
25
0.00
0.05
0.10
0.15
(d)
Total(d_{MRG})
Shift(d_S)
Equilibrium(d_E)
Density
0
5
10
15
20
25
30
35
0.00
0.05
0.10
0.15
Index value

Table 1. Summary of indices, formulae, and references citing indices developed in previous studies and proposed in this study. y_{ij} is abundance excluding individuals (i.e., measures or weights) of species *i* at time T*j* at a site, and y_{ik} is abundance excluding individuals of species *i* at time T*k* at a site.

Index	Formula	References
d_{BC}	$\frac{B+C}{2A+B+C} = \frac{\sum_i[x_{ij} - \min(x_{ij}, x_{ik})] + \sum_i[x_{ik} - \min(x_{ij}, x_{ik})]}{2[\sum_i \min(x_{ij}, x_{ik})] + \sum_i[x_{ij} - \min(x_{ij}, x_{ik})] + \sum_i[x_{ik} - \min(x_{ij}, x_{ik})]}$	Odum (1950)
d_{mr}	$\frac{m+r}{2p+m+r} = \frac{\sum_o[z_{oj} - \min(z_{oj}, z_{ok})] + \sum_o[z_{ok} - \min(z_{oj}, z_{ok})]}{2[\sum_o \min(z_{oj}, z_{ok})] + \sum_o[z_{oj} - \min(z_{oj}, z_{ok})] + \sum_o[z_{ok} - \min(z_{oj}, z_{ok})]}$	Nakadai (2020)
$v_{s.QL}$	$\frac{B+C}{2e+B+C} = \frac{B+C}{m+r} = \frac{\sum_i[x_{ij} - \min(x_{ij}, x_{ik})] + \sum_i[x_{ik} - \min(x_{ij}, x_{ik})]}{2[\sum_i \min(x_{ij}, x_{ik}) - \sum_o \min(z_{oj}, z_{ok})] + \sum_i[x_{ij} - \min(x_{ij}, x_{ik})] + \sum_i[x_{ik} - \min(x_{ij}, x_{ik})]}$	Nakadai (2020)
$d_{BC'}$	$\frac{B'+C'}{2A'+B'+C'} = \frac{\sum_i[y_{ij} - \min(y_{ij}, y_{ik})] + \sum_i[y_{ik} - \min(y_{ij}, y_{ik})]}{2[\sum_i \min(y_{ij}, y_{ik})] + \sum_i[y_{ij} - \min(y_{ij}, y_{ik})] + \sum_i[y_{ik} - \min(y_{ij}, y_{ik})]}$	Odum (1950)

d_{MRG}	$\frac{M+R+G}{2P+M+R+G} = \frac{\sum_o \left[w_{oj} - \min(w_{oj}, w_{ok}) \times \left[z_{oj} - \min(z_{oj}, z_{ok})\right]\right] + \sum_o \left[\left[w_{ok} - \min(w_{oj}, w_{ok})\right] \times \left[z_{ok} - \min(z_{oj}, z_{ok})\right]\right] + \sum_o \left[\left[\max(w_{oj}, w_{ok}) - \min(w_{oj}, w_{ok})\right] \times \min(z_{oj}, z_{ok})\right]}{2[\sum_o \min(w_{oj}, w_{ok}) + \sum_o \left[w_{oj} - \min(w_{oj}, w_{ok}) \times \left[z_{oj} - \min(z_{oj}, z_{ok})\right]\right] + \sum_o \left[\left[w_{ok} - \min(w_{oj}, w_{ok})\right] \times \left[z_{ok} - \min(z_{oj}, z_{ok})\right]\right] + \sum_o \left[\left[\max(w_{oj}, w_{ok}) - \min(w_{oj}, w_{ok})\right] \times \min(z_{oj}, z_{ok})\right]}$	This study
$v_{s.QT}$	$\frac{B'+C'}{2E+B'+C'} = \frac{\sum_i \left[y_{ij} - \min(y_{ij}, y_{ik})\right] + \sum_i \left[y_{ik} - \min(y_{ij}, y_{ik})\right]}{2[\sum_i \min(y_{ij}, y_{ik}) - \sum_o \min(w_{oj}, w_{ok})] + \sum_i \left[y_{ij} - \min(y_{ij}, y_{ik})\right] + \sum_i \left[y_{ik} - \min(y_{ij}, y_{ik})\right]}$	This study

Table 2. Results of a multi-regression model based on the best models selected using an Akaike information criterion (AIC) comparison for individual-based qualitative and quantitative beta-diversity indices. *β* and *parR2* indicate the regression coefficients and partial adjusted *R*-squared values of each explainatory variable, respectively. *Adj R2* is the adjusted *R*-squared value for the complete model. Note: Significance: .<0.1, *<0.05, **<0.01, ***<0.001. When a null model was chosen, † is added into the column of p-value for whole model.

	Latitude				Elevation				Calendar year				Survey interval				*Adj R2*	*P-values*	
	β	*parR2*	*P-values*		β	*parR2*	*P-values*		β	*parR2*	*P-values*		β	*parR2*	*P-values*				
(a) Qualitative-family indices																			
d_{BC}	–	–	–		–	–	–		–	–	–		–	–	–			†	
d_{mr}	–	–	–		–	–	–		–	–	–		0.0186	0.0089	0.1473		0.0089	0.1473	
d_m	-0.0807	0.0333	0.0233	*	–	–	–		0.0098	0.0953	0.0003	***	–	–	–		0.1211	0.0001	***
dr	–	–	–		–	–	–		-0.0129	0.0513	0.0064	**	0.0277	0.0146	0.0944	.	0.0554	0.0111	*
$v_{s.QL}$	–	–	–		0.0002	0.0283	0.0393	*	–	–	–		–	–	–		0.0283	0.0393	*
(b) Qantitative-family indices																			
(i) Basal area																			
$d_{BC'}$	–	–	–		–	–	–		–	–	–		–	–	–			†	
d_{MRG}	-0.0705	0.0095	0.1413		–	–	–		–	–	–		0.0231	0.0192	0.0663	.	0.0269	0.0695	.
d_M	-0.0768	0.0253	0.0421	*	–	–	–		0.0094	0.0770	0.0010	**	–	–	–		0.0972	0.0007	***
d_R	–	–	–		–	–	–		-0.0044	0.0259	0.0398	*	–	–	–		0.0259	0.0398	*
d_G	–	–	–		–	–	–		-0.0028	0.0236	0.0477	*	0.0122	0.0381	0.0165	*	0.0305	0.0553	.
$v_{s.QT}$	–	–	–		–	–	–		–	–	–		–	–	–			†	
(ii) Bole biomass																			
$d_{BC'}$	–	–	–		–	–	–		–	–	–		0.0205	0.0114	0.1210		0.0114	0.1210	
d_{MRG}	-0.0748	0.0094	0.1429		–	–	–		–	–	–		0.0278	0.0264	0.0387	*	0.0336	0.0454	*
d_M	-0.0766	0.0209	0.0586	.	–	–	–		0.0092	0.0641	0.0026	***	–	–	–		0.0812	0.0020	**
d_R	–	–	–		–	–	–		-0.0039	0.0187	0.0684	.	–	–	–		0.0187	0.0685	.
d_G	–	–	–		–	–	–		–	–	–		0.0089	0.0227	0.0503	.	0.0227	0.0503	.
$v_{s.QT}$	–	–	–		–	–	–		-0.0301	0.0272	0.0366	*	0.0717	0.0082	0.1569		0.0232	0.0877	.

Appendices

Table S1. Comparison using a linear and linear mixed model for each index. The best models chosen from the comparison are shown in Table 2

Figure S1. Map of geographic locations of plots included in the subset of the Forest Inventory and Analysis (FIA) database for the state of Rhode Island in USA (Stanke et al., 2020). Sites with darker colour points have multiple survey intervals.

Figure S2. Density plots representing the distribution of individual-based quantitative beta-diversity indices across 126 survey intervals of 86 plots (data from Stanke et al., 2020). In the right four plots (b, d, f, and h), the index values are limited to the range 0–0.15 to enable comparison (also see Fig. 2). In the left four plots, the entire value is shown. Plots (a), (b), (e), and (f) are based on basal area, and plots (c), (d), (g), and (h) are based on bole biomass.

Figure S3. Correlations among the calculated indices.

Supplementary text 1. Explanation of individual-based temporal beta diversity employing the Ružička dissimilarity index.

Supplementary file 1. R software script for individual-based temporal beta diversity calculations using sample data.